Polymer, 55(9), 2213-2219 (2014).

Nanostructured Poly(3-hexylthiophene-2,5-diyl) Films with Tunable Dimensions through Self-Assembly with Polystyrene

Varun Vohra[a,*], *Osamu Notoya*[b], *Tong Huang*[a], *Masayuki Yamaguchi*[a], *Hideyuki Murata*[a,*]

[a] School of Materials Science, Japan Advanced Institute of Science and Technology,

1-1 Asahidai, Nomi, Ishikawa 923-1292, Japan

[b] Nano-material Technology Center, Japan Advanced Institute of Science and Technology,

1-1 Asahidai, Nomi, Ishikawa 923-1292, Japan

*Email: varunvohra1984@gmail.com (V.Vohra)

murata-h@jaist.ac.jp (H. Murata)

Abstract:

Poly(3-hexylthiophene-2,5-diyl) is among the most widely used conjugated polymers for opto-electronic applications. To enhance its properties, researchers have attempted to nanostructure this polymer using various processes including breath figure arrays, nanolithography and elaborated organic synthesis. We here demonstrate a simple process to nanostructure the conjugated polymer using self-assembly with polystyrene and selective removal of one of the phases. The influence of the molecular weight of each polymer on the thin film morphology was systematically studied by atomic force microscopy. Using this approach, we observe two types of nanostructure, namely, nanoporous and nanoisland structures, of which the dimensions can be tuned by modifying the molecular weight of each polymer in the blend. This simple process introduces a cost-effective alternative to produce thin films of conjugated polymer with average nano-features from 100 nm up to 500 nm which could be used in a wide range of applications.

Keywords: self-assembly; nanostructure; conjugated polymer

Introduction:

Poly(3-hexylthiophene-2,5-diyl) (P3HT) has been extensively used in the past decade by researchers working in the fields of organic photovoltaics,[1,2] field effect transistors[3,4] and sensors.[5,6] Previous works have demonstrated that nanostructuration of P3HT can be beneficent in such devices as it not only provides a larger interface between P3HT and other materials or air but also because the P3HT chain can rearrange due to nanoconfinement.[7-9] Various processes have been used to produce nanostructured P3HT thin films. These include, among others, the use of breath figure arrays,[10] self-assembly using block or branched copolymers[11-13] and soft lithography using nanostructured molds such as nanoporous alumina.[14] Each of these techniques presents some drawbacks either in term of cost of production or properties of the thin films. More specifically, the breath figure array technique is a very simple and cost-effective technique with which porous structures with pore diameters in the range of 600 nm to micrometer scale can be easily produced. However, it is fairly difficult to reduce the pore diameters below 600 nm and, as it consists of a drop casting technique, the film thickness cannot be controlled. The use of block copolymers is very efficient to produce nanostructures of conjugated polymers but the complicated chemistry as well as the difficulties encountered to separate the conjugated and insulating parts of the films may lead to poor device performances.[11-13] Nanoimprinting is very efficient and allows the formation of various nanostructures but presents major drawbacks in terms of cost of production and control or optimization of the process variables (time, temperature and pressure applied for the nanoimprinting process).[14]

We recently introduced a technique based on the formation of self-assembled thin spin-coated films of P3HT blended with polystyrene (PS).[9] During the spin-coating process, the two polymers phase separate leading to the formation of various structures including nanoporous (at low PS concentrations) and nanoisland (at high PS concentrations) structures. As P3HT and PS

have different dispersive and polar components of the solubility parameters, we are able to selectively remove PS from the films without damaging the P3HT nanostructures using the adequate solvent. As this approach, represented in **Figure 1**, may also be applied to other P3HT:polymer blends, we first verify that P3HT:PS is the most adequate system by comparing the thin film morphologies obtained upon blending P3HT with PS, poly(methyl methacrylate) (PMMA) or poly(ethylene oxide) (PEO). Consequently, through a systematic morphological study using atomic force microscopy (AFM), we observe the influence of the weight-average molecular weight (Mw) of both P3HT and PS on the resulting structures for high and low P3HT concentrations. This study, which is complementary to our previous work focusing on the influence of the P3HT:PS weight ratio, demonstrates that by changing the Mw, we can produce nanostructured thin films of P3HT with tunable dimensions. More specifically, in the case of both nanoporous and nanoisland structures, the average diameters of the features can be tuned from around 100 nm up to 500 nm. The dimensions of the nanostructures obtained in this work therefore perfectly fill the gap between the small diameter porous alumina (30 to 150 nm)[14] and the large diameter breath figure arrays (from 600 nm up to a few microns).[10] Furthermore, these nanostructured thin films provide a simple method which can easily be integrated in organic electronics and sensing devices fabrication.[5,7-10]

Experimental:

P3HT was purchased from Merck and PS, PMMA and PEO from Sigma Aldrich. We selected two P3HT, respectively a low ($P3HT_{LMW}$) and a high molecular weight P3HT ($P3HT_{HMW}$) to be combined with either PS, PMMA or PEO. Three different types of PS were used in the experiments, namely, a low (PS_{LMW}), medium (PS_{MMW}) and high molecular weight PS (PS_{HMW}).

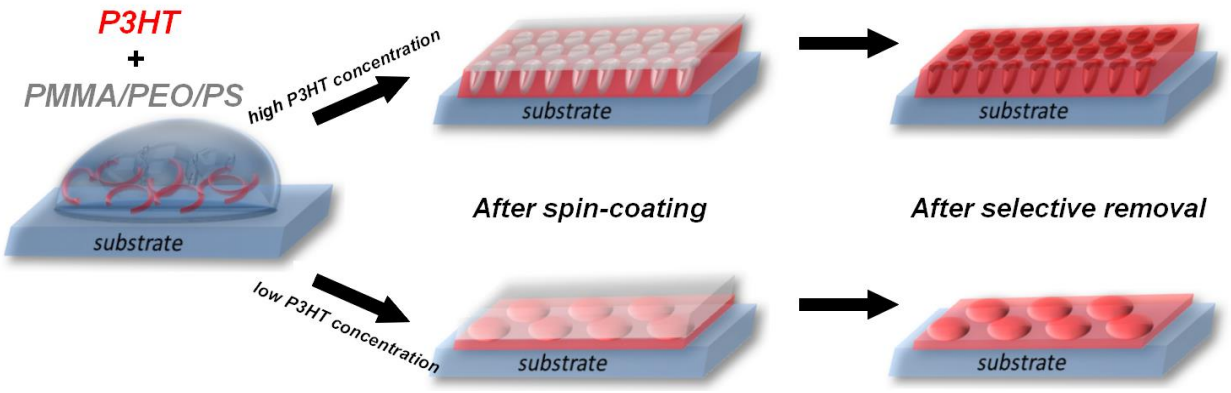

Figure 1. Schematic representation of the expected formation of nanoporous and nanoisland films at various steps of the fabrication process.

Table 1 summarizes the molecular weights for the various polymers used in this study where Mn, Mw and PDI correspond respectively to the number average molecular weight, the weight average molecular weight and the polydispersity index. The molecular weight and its distribution were evaluated by a gel permeation chromatography (GPC) (Tosoh, HLC-8020) with TSK-GEL GMHXL as a polystyrene standard. Chloroform was employed as eluant at a flow rate of 1.0 ml/min, and the sample concentration was 0.5 mg/ml. PEO could not be characterized using GPC and therefore the viscosity average molecular weight (Mv) information corresponds to the one provided by the supplier.

polymer	***$P3HT_{LMW}$***	***$P3HT_{HMW}$***	***PS_{LMW}***	***PS_{MMW}***	***PS_{HMW}***	***PMMA***	***PEO***
Mn	10 030	49 200	1 810	1 750	70 670	35 610	-
Mw	20 050	197 500	1 880	28 010	283 380	75 950	-
PDI	2.00	4.01	1.04	16.0	4.01	2.13	-
Mv	-	-	-	-	-	-	400 000

Table 1: Summary of average molecular weights and polydispersity index (PDI) of the various polymers.

The blend solutions were prepared at a concentration of 30mg/ml in chlorobenzene. The solutions were stirred at 50°C for 1 hour prior to spin-coating to ensure that all materials are well dissolved. Glass substrates were cleaned following a regular cleaning procedure and then placed in a UV-O_3 surface treatment apparatus for 30 min. For scanning electron microscopy (SEM) measurements, ITO covered glass substrates were prepared following the same procedure. The solutions were spin-coated on the 2.5 cm x 2.5 cm surface treated substrates at 2000 rpm for 60 s. The samples demonstrate similar nanostructures over the entire area of the substrates (excluding a very small area close to the edge where deformed structures can be observed). An example of larger scale (100 μm x 100 μm) AFM image can be found in the Supporting Information (**Figure SI1**). The typical thickness obtained prior to non-P3HT phase removal vary between 140 and 230 nm. We observe a decrease of the total thickness in all cases which depends on the polymer combination used and the weight ratio of P3HT and varies between 30 nm up to 150 nm (taken from the parts of the films in between two successive pores or islands).

For selective removal of PS and PMMA from the thin films, the substrates were soaked into acetone for 30 min and the surface was further cleaned with acetone to ensure complete removal from the surface. Similarly, for PEO, we use acetonitrile. The surface morphology was analyzed using an AFM from Keyence (Nanoscale Hybrid Microscope VN-8000).

Results and discussion:

The general terms of the solubility parameter (δ) of P3HT, PS, PMMA and PEO are 20.0, 22.5, 22.6 and 22.1 $MPa^{1/2}$, respectively.[15,16] As the value of δ for chlorobenzene is 19.58 $MPa^{1/2}$, all these polymers can easily be dissolved in chlorobenzene. However, it is worth noticing that, for example, even though P3HT seems to be more soluble in chlorobenzene from a theoretical point of view, the critical concentration of PS at room temperature is much higher than one of P3HT.

Although all polymers are soluble in chlorobenzene, they are not completely miscible with each other which is at the origin of the formation of phase segregated thin films. Moreover, unlike their general solubility parameter, the dispersive, dipolar and hydrogen bonds components of the solubility parameters of the polymers are rather different, which results in the possibility of selectively removing PS, PMMA and PEO from the blend films using the adequate solvent and explains the immiscibility of the various polymer:polymer combinations (**Table 2**).

solubility parameter $(MPa^{1/2})$	δ_T	δ_d	δ_p	δ_H
P3HT	20.0	18.5	5.3	5.3
PS	22.5	21.3	5.8	4.3
PMMA	22.6	18.6	10.5	7.5
PEO	22.1	17.0	11.0	8.9

Table 2: Hansen solubility parameters of the various polymers.[15,16]

We first compare the morphologies obtained with these polymers combined with P3HT. Blends of P3HT with PS, PMMA or PEO with various P3HT concentrations were studied and Figure 2 displays representative morphologies obtained for each combination of polymers after removal of the non-P3HT phase. Although various blend ratios were prepared for the three different systems, the images shown here correspond to the optimized blend ratio to produce nanoporous structures (when possible).

We clearly observe that porous morphologies can be fabricated with both PS and PMMA. However, we were unable to produce nanoisland structures with the P3HT:PMMA blends. Furthermore, the nanoporous structures obtained with PMMA are less organized than the nanoporous films resulting from P3HT:PS blends. P3HT:PEO, on the other hand, does not result in the formation of any nanostructured films after removal of PEO and only surface roughness from the crystaline P3HT can be observed. The change in film thickness observed upon selective

removal of PEO suggests the formation of vertically segregated bilayer morphology. Some peculiar formations of PEO on P3HT can also be observed in some cases (**Figure SI2**, Supporting Information) confirming that the two polymers segregate very strongly even though their general solubility parameter terms are the closest among the three blend systems.

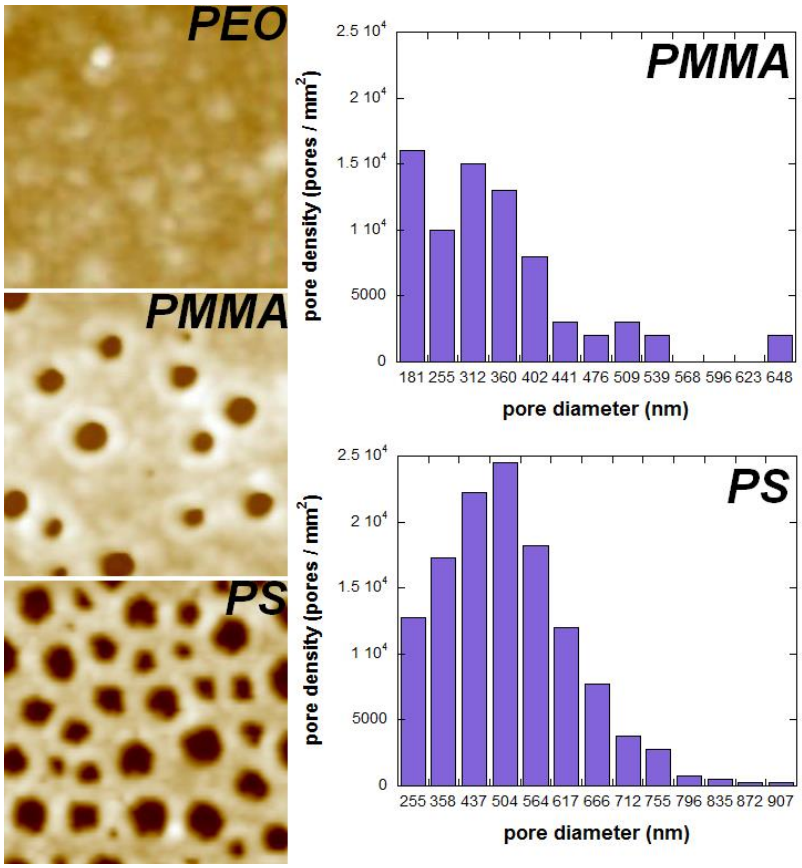

Figure 2. Representative morphologies obtained by blending $P3HT_{HMW}$ with PEO (35 wt%), PMMA (20 wt%) or PS_{HMW} (50 wt%) after removal of non-P3HT phase. The AFM images correspond to an area of 5μm x 5μm. The histograms (right) were calculated using 20 μm x 20 μm images to obtain information about the pore size distribution.

The dispersive components of PMMA and P3HT, as well as the polar and hydrogen components of PS and P3HT are very close to each other while all three components of the solubility parameter of PEO and P3HT differ. The dispersive component may be at the origin of the partial

compatibility of PMMA with P3HT leading to the porous structures. As PS has two solubility parameter components similar to P3HT, the increased compatibility of the two polymers results in the fabrication of much more defined structures with higher pore densities compared to the P3HT:PMMA blends (**Figure 2**).

The P3HT:PS system therefore seems to be the most adequate combination for fabricating both nanoisland and nanoporous ordered thin films. In consequence, we will focus our study on this particular combination of materials.

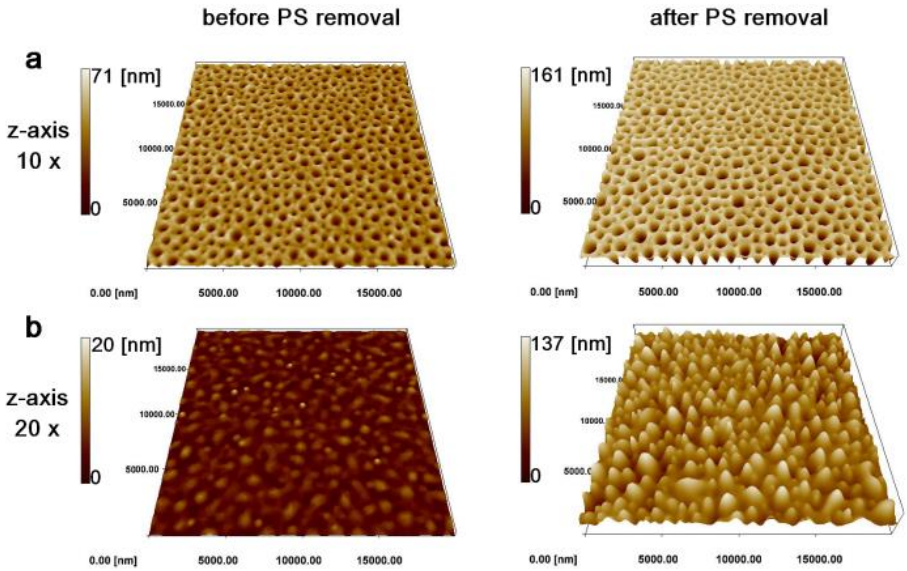

Figure 3. Examples of porous (a) and island (b) structures before (left) and after (right) PS removal using acetone. The porous structure was obtained using a $P3HT_{HMW}$:PS_{MMW} blend with a 1:1 ratio while the island structure results from a $P3HT_{HMW}$:PS_{HMW} blend composed of 85 PS wt%. The 3D AFM images correspond to an area of 20μm x 20μm.

Figure 3 presents the two types of structure obtained from high and low P3HT concentrations before and after selective removal of PS with acetone. From these AFM images we can observe that the nanostructuration of P3HT is likely obtained prior to PS removal. However, the structure is enhanced after selective removal of PS, especially in the case of the nanoisland structures. This

reveals that PS forms a thin layer at the P3HT/air interface and that the polymers not only segregate in the plane of the substrate but also in the vertical direction with P3HT being pushed down close to the substrate. This phenomenon may be related to the lower solubility of P3HT in chlorobenzene. As spin-coating is a fast drying process, the structures obtained prior to PS removal do not necessarily correspond to the thermodynamic equilibrium. To verify whether the thermal equilibrium was achieved, we collected images of the structures before and after applying various annealing temperatures (over the glass transition temperatures and the melting temperatures of the polymers). These results (**Figure SI4**, Supporting Information) suggest that the pristine films after spin-coating are in a kinetic state and have not achieved the thermal equilibrium. Even though, annealing over the glass transition temperature does not lead to major morphological changes, annealing over the melting temperature of both polymers (even for a short time) increases drastically the vertical phase segregation.

With the objective of understanding the influence of the Mw on the formed structures, we selected two P3HT which will be referred to as $P3HT_{LMW}$ and $P3HT_{HMW}$. These P3HT were associated with three PS, namely, PS_{LMW}, PS_{MMW} and PS_{HMW}. **Table SI1** (Supporting Information) summarizes the analysis of the structures observed for 25, 50 and 75 wt% of PS for all the P3HT/PS combinations.

The miscibility of two polymers can be described using the Gibb's free energy of mixing ΔG_{mix} which is composed of two terms: the enthalpy of mixing (ΔH_{mix}) and the entropic contribution corresponding to $T\Delta S_{mix}$. Complete miscibility of two polymers can only be obtained if ΔG_{mix} is negative. The value of $T\Delta S_{mix}$ is always positive as there is always an increase in the entropy upon mixing. The mixing enthalpy can be estimated using the Flory-Huggins interaction parameter (χ) which takes into account the contact energy between the different polymers as well

as the contact energy between different molecules of the same polymer.[17,18] It is worth mentioning that the molecular weight of the polymer chains does not remarkably affect the interaction parameter. The interaction parameter for P3HT and PS blends at 150°C has been previously reported to be 0.6.[19] Assuming that the interaction parameter is proportional to 1/T, we can extrapolate the value of χ at room temperature for P3HT/PS mixtures to be 0.85.

The Flory-Huggins model respectively describes the enthalpy and entropy of mixing as: [17,18]

$$\Delta H_{mix} = RTV\,\varphi_1\varphi_2\,\chi \qquad \text{(Eq. 1)}$$

$$-T\Delta S_{mix} = RTV\left(\frac{\rho_1\varphi_1}{M_1}\ln\varphi_1 + \frac{\rho_2\varphi_2}{M_2}\ln\varphi_2\right) \qquad \text{(Eq. 2)}$$

where R is the gas constant, T the temperature, V the total volume and where ρ, ϕ and M are the density, the volume fraction and molecular weight of each material, respectively.

The Gibb's free energy of mixing can therefore be expressed as:

$$\Delta G_{mix} = RTV\left(\varphi_1\varphi_2\,\chi + \frac{\rho_1\varphi_1}{M_1}\ln\varphi_1 + \frac{\rho_2\varphi_2}{M_2}\ln\varphi_2\right) \qquad \text{(Eq. 3)}$$

As the enthalpic contribution is independent of the molecular weight, the changes observed in phase separation behavior upon variation of the Mw of the polymers are mainly related to the entropic contribution to the free energy of mixing. It should be kept in mind that the entropic and enthalpic contributions are of opposite sign and that the enthalpic contribution is larger than the entropic contribution. In fact, the entropy only contributes to the Gibb's free energy of mixing at low Mw. In the case of P3HT/PS blends, this results in an overall lower value of the Gibb's free

energy and better mixing when using low Mw polymers (when 1/M is no longer negligible).

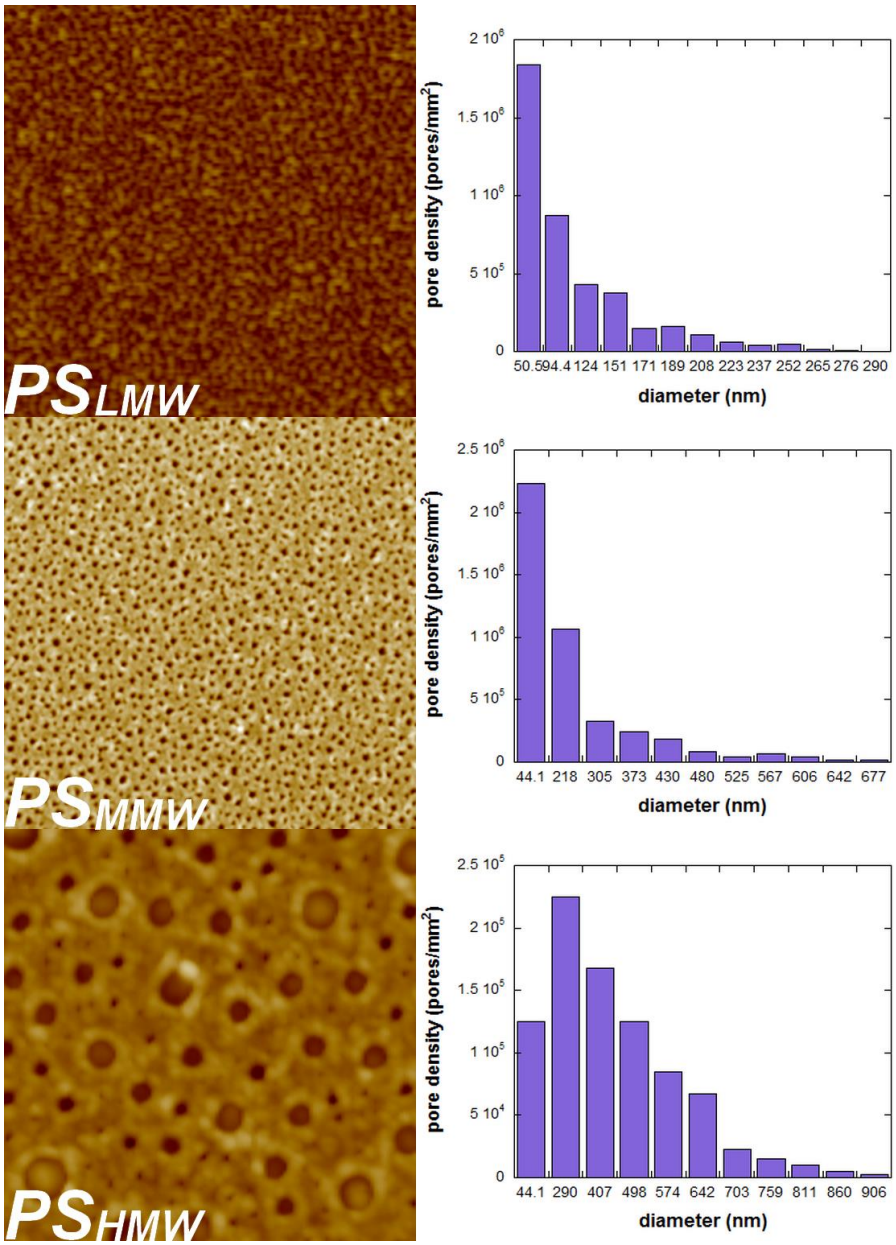

Figure 4. Pore diameters increasing with PS Mw (blended with $P3HT_{LMW}$). The composition of the polymer blend is kept constant at 25 wt% of PS. The AFM images correspond to an area of 10μm x 10μm. The histograms (right) were calculated using 20 μm x 20 μm images to obtain information about the pore size distribution.

The AFM images in **Figure 4** visually confirm the larger phase separation with increasing Mw of PS. In fact, we have studied the influence of the Mw of PS on nanopore formation by fixing the PS content to 25 wt%. We then combine the various PS with $P3HT_{LMW}$ and observe the influence on the pore formation and dimensions. When using PS_{LMW}, the porous structure is barely formed while on the other hand, PS_{MMW} and PS_{HMW} show a nice nanoporous formation with average pore diameters of 167 and 295 nm respectively. The influence of PS Mw is therefore quite obvious and as predicted by the Flory-Huggins model, with a given P3HT and composition, increasing Mw leads to a larger Gibb's free energy of mixing and consequently, a widening of the pore dimensions.

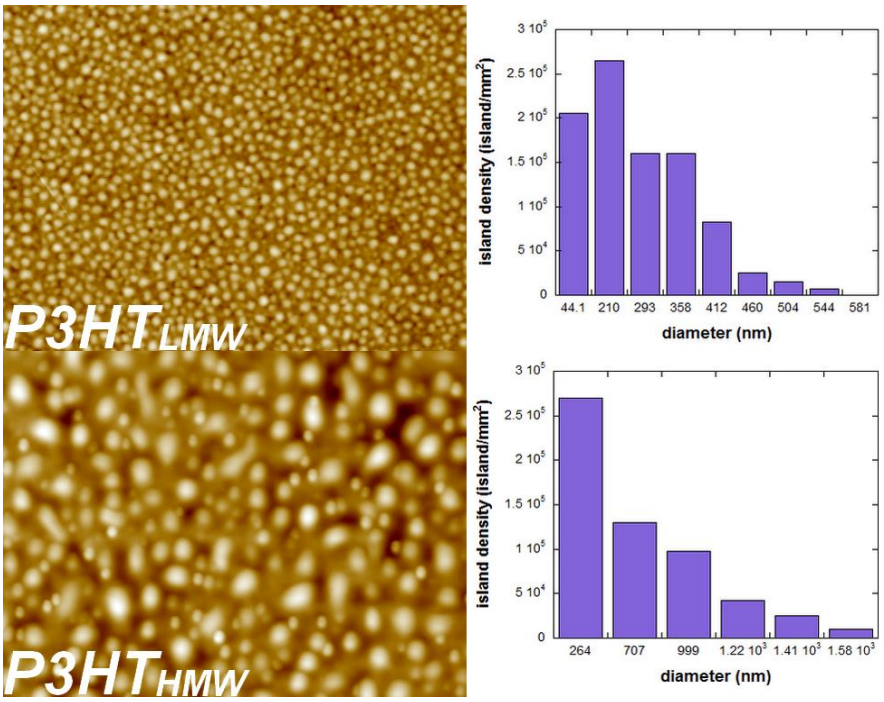

Figure 5. Island dimensions increasing with P3HT Mw (blended with PS_{HMW}). The composition of the polymer blend is kept constant at 85 wt% of PS. The AFM images correspond to an area of 20μm x 15μm. The histograms (right) were calculated using 20 μm x 20 μm images to obtain information about the island size distribution.

Similarly, **Figure 5** presents the evolution of the island dimensions by increasing the P3HT Mw at a fixed PS concentration of 85 wt%. The influence of the one order of magnitude change in Mw is clearly observed: a large increase in island diameter when replacing $P3HT_{LMW}$ with $P3HT_{HMW}$. Comparably to what could be observed in Figure 4, the island dimensions are much more monodisperse in the case of low Mw compared to high Mw. The nanoislands obtained with $P3HT_{LMW}$ have an average diameter of 233 nm while the ones produced using $P3HT_{HMW}$ are 371 nm wide in average with diameters ranging from 264 to 1580 nm and a much less organized structure.

With this simple and cost-effective process, we have demonstrated that the Mw of each of the polymers used in the blend can provide means to control the dimensions of the nanostructured produced and a wide range of pore dimensions can be obtained.

Conclusions:

The process we introduced in a previous study represents a cost-efficient alternative to the existing methods to nanostructure P3HT. However, we have demonstrated that this approach cannot be generalized to blends of P3HT with any other matrix polymers such as PMMA or PEO. The peculiar morphologies observed are therefore a consequence of the specific interactions between P3HT and PS. The fabrication method based on blends of P3HT:PS which we designed produces two types of nanostructures: nanoporous and nanoislands films. The induced phase separation resulting from repulsive interactions between the two polymers allows for selective removal of PS using acetone leaving the nanostructured P3HT films undamaged. Not only have we confirmed that the influence of the blend composition on the morphology occurs for practically any Mw in blends of these two polymers, but we have also demonstrated that the Mw has a major influence on the dimensions of the nanostructures obtained.

We further confirmed that the influence of the Mw on the formed structures results from a larger contribution of the entropy to the Gibb's free energy at low Mw. By combining the Mw effect to the PS composition in the blends, we have the possibility to tune average pore diameters from about 100 nm up to over 500 nm. This method therefore offers a cost-effective process which is complimentary to breath figure formation and nanoporous alumina in terms of dimensions obtained. Moreover, breath figure arrays and anodic alumina only produce porous structures and we can also fabricate the negative structures (islands) using the polymer self-assembly approach. These few hundreds of nanometers thick spin-coated films make ideal candidates for use in opto-electronic and sensing devices.

Acknowledgements:

The work was supported by a Grant-in-Aid for Scientific Research on Innovative Areas (No. 20108012, "pi-Space") from the Ministry of Education, Culture, Sports, Science, and Technology, Japan. V. Vohra would like to greatly acknowledge financial support through research fellowships from the Japan Society for Promotion of Science for postdoctoral fellowships for foreign researchers.

References:

(1) Chen, D.; Nakahara, A.; Wei, D.; Nordlund, D.; Russell, T. P. P3HT/PCBM Bulk Heterojunction Organic Photovoltaics: Correlating Efficiency and Morphology. *Nano Lett.* **2011**, *11*, 561-567.

(2) Dennler, G.; Scharber, M. C.; Brabec, C. J. Polymer-Fullerene Bulk-Heterojunction Solar Cells. *Adv. Mater.* **2009**, *21*, 1323-1338.

(3) Park, Y. D.; Lim, J. A.; Lee, H. S.; Cho, K. Interface Engineering in Organic Transistors. *Mater. Today* **2007**, *10*, 46-54.

(4) Majewski, L. A.; Kingsley, J. W.; Balocco, C.; Song, A. M. Influence of Processing Conditions on the Stability of Poly(3-hexylthiophene)-based Field-effect Transistors. *Appl. Phys. Lett.* **2006**, *88*, 222108.

(5) Khot, L. V.; Panigrahi, S.; Sengupta, P. Development and Evaluation of Chemoresistive Polymer Sensors for Low Concentration Detection of Volatile Organic Compounds Related to Food Safety Applications. *Sens. & Instrumen. Food Qual.* **2010**, *4*, 20–34.

(6) Scarpa, G.; Idzko, A.-L.; Yadav, A.; Thalhammer, S. Organic ISFET Based on Poly (3-hexylthiophene). *Sensors* **2010**, *10*, 2262-2273.

(7) Aryal, M.; Trivedi, K.; Hu, W. Nano-Confinement Induced Chain Alignment in Ordered P3HT Nanostructures Defined by Nanoimprint Lithography. *ACS Nano* **2009**, *3*, 3085-3090.

(8) Jo, S. B.; Lee, W. H.; Qiu, L.; Cho, K. Polymer Blends with Semiconducting Nanowires for Organic Electronics. *J. Mater. Chem.* **2012**, *22*, 4244-4260.

(9) Vohra, V.; Campoy- Quiles, M.; Garriga, M.; Murata, H.; Organic Solar Cells Based on Nanoporous P3HT Obtained from Self-assembled P3HT:PS Templates. *J. Mater. Chem.* **2012**, *22*, 20017-20025.

(10) Vohra, V.; Yunus, S.; Attout, A.; Giovanella, U.; Scavia, G.; Tubino, R.; Botta, C.; Bolognesi, A. Bifunctional Microstructured Films and Surfaces Obtained by Soft Lithography from Breath Figure Arrays. *Soft Matter* **2009**, *5*, 1656-1661.

(11) Sivanandan, K.; Chatterjee, T.; Treat, N.; Kramer, E. J.; Hawker, C. J. High Surface Area Poly(3-hexylthiophenes) Thin Films from Cleavable Graft Copolymers. *Macromolecules* **2010**, *43*, 233–241.

(12) Han, X.; Chen, X.; Holdcroft, S. Nanostructured Morphologies and Topologies of π-Conjugated Polymers from Thermally Reactive Polymer Blends. *Adv. Mater.* **2007**, *19*, 1697‑1702.

(13) Takahashi, A.; Rho, Y.; Higashihara, T.; Ahn, B.; Ree, M.; Ueda, M.; Preparation of Nanoporous Poly(3-hexylthiophene) Films Based on a Template System of Block Copolymers via Ionic Interaction. *Macromolecules* **2010**, *43*, 4843–4852.

(14) Aryal, M.; Buyukserin, F.; Mielczarek, K.; Zhao, X.-M.; Gao, J.; Zakhidov, A.; Hu, W. Imprinted Large-scale High Density Polymer Nanopillars for Organic Solar Cells. *J. Vac. Sci. Technol. B* **2008**, *26*, 2562-2566.

(15) Machui, F.; Abbott, S.; Waller, D.; Koppe, M.; Brabec, C. J. Determination of Solubility Parameters for Organic Semiconductor Formulations. *Macromolec. Chem. Phys.* **2011**, *212*, 2159–2165.

(16) Brandrup, J., Immergut, E. H., Grulke, E. A., Abe, A., Bloch, D. R. *Polymer Handbook*, 4th Edition. Eds. John Wiley and Sons, New York **1999**.

(17) Huggins, M. L. Solutions of Long Chain Compounds. *J. Chem. Phys.* **1941**, *9*, 440.

(18) Flory, P. J. Thermodynamics of High Polymer Solutions. *J. Chem. Phys.* **1941**, *9*, 660.

(19) Lee, Y.; Kim, J. K.; Chiu, C.-H.; Lan, Y.-K.; Huang, C.-I. Phase Behavior of Poly(3-alkylthiophene)/Polystyrene Blends. *Polymer* **2009**, *50*, 4944-4949.